nature materials

LETTERS

PUBLISHED ONLINE: 3 FEBRUARY 2013 | DOI: 10.1038/NMAT3553

# Domain wall depinning governed by the spin Hall effect

P. P. J. Haazen*, E. Murè, J. H. Franken, R. Lavrijsen, H. J. M. Swagten and B. Koopmans

**Perpendicularly magnetized materials have attracted significant interest owing to their high anisotropy, which gives rise to extremely narrow, nanosized domain walls. As a result, the recently studied current-induced domain wall motion (CIDWM) in these materials promises to enable a new class of data, memory and logic devices[1–5]. Here we propose the spin Hall effect as an alternative mechanism for CIDWM. We are able to carefully tune the net spin Hall current in depinning experiments on Pt/Co/Pt nanowires, offering unique control over CIDWM. Furthermore, we determine that the depinning efficiency is intimately related to the internal structure of the domain wall, which we control by the application of small fields along the nanowire. This manifestation of CIDWM offers an attractive degree of freedom for manipulating domain wall motion by charge currents, and sheds light on the existence of contradicting reports on CIDWM in perpendicularly magnetized materials[6–11].**

Current-induced domain wall motion (CIDWM) is often explained in terms of the adiabatic and non-adiabatic torques[12–15], which both depend on the in-plane spin current that arises from the spin polarization of the charge current that runs in the ferromagnet. However, in the typical multilayer structures used for domain wall motion in perpendicular materials, a second spin current, generated by the spin Hall effect (SHE) in the adjacent non-magnetic metal layers[16–18], can be injected into the ferromagnet. Materials exhibiting a large SHE are often used for these non-magnetic metal layers, because both the perpendicular anisotropy and the SHE depend strongly on spin–orbit coupling. In such multilayered thin films, the SHE is particularly efficient in affecting the magnetization because of its large injection interface (the in-plane cross-section of the wire). In these structures, spin Hall currents have indeed been shown to change the effective damping[19], induce ferromagnetic resonance[20], inject and detect spin waves[21], and switch the magnetization of in-plane magnetized β-Ta/CoFeB (ref. 22) and out-of-plane magnetized Pt/Co/$AlO_x$ (refs 23,24) nanodots. Furthermore, it was suggested that CIDWM in in-plane materials could be influenced[25]. These considerations suggest that the SHE plays an important role in the intensively studied CIDWM in perpendicular materials. Here, we explore the potential of CIDWM by the SHE, showing that it in fact constitutes the main contribution to domain wall motion in Pt/Co/Pt.

To study the effect of the spin Hall current on domain wall motion, we have used Pt/Co/Pt structures. Both Pt layers in this stack act as a spin Hall current source, which inject oppositely oriented spins into the ferromagnetic Co layer (Fig. 1a). Therefore, to inject a net spin current into the Co, the spin Hall currents from the two Pt layers should not cancel fully. This is achieved by choosing unequal Pt layer thicknesses in the range of the spin diffusion length of Pt, because the spin Hall current is dependent on the layer thickness, as was experimentally verified previously[20]. Pt/Co/Pt stacks have the further advantage that Rashba effects are negligible. In the closely related Pt/Co/$AlO_x$, in which SHE-induced magnetization reversal has been shown recently[23,24], it was suggested that a non-adiabatic contribution of the Rashba field[26] could be important. In Pt/Co/Pt, there are two approximately equal (Pt/Co) interfaces, resulting in a Rashba field that is negligible (see Supplementary Information for experimental backup). Pt/Co/Pt therefore functions as an excellent model system to unambiguously study the hitherto unexplored role of the SHE in domain wall dynamics.

First, we have verified that the SHE can indeed inject a net spin current, capable of inducing a significant torque on the magnetization, into an asymmetric Pt (4 nm)/Co (0.5 nm)/Pt (2 nm) nanowire. For these unequal Pt layer thicknesses, the net spin Hall current should be approximately 35% of the bulk value[27]. As confirmation, we have performed pure current-induced switching of a uniformly magnetized nanowire, analogous to experiments performed on Pt/Co/$AlO_x$ (refs 23,24). Current pulses of 30 ns and $5 \times 10^{11}$ A m$^{-2}$ were injected into a nanowire subjected to an applied field, $\mu_0 H_x = 20$ mT, parallel to the charge current. Indeed, the current pulses result in magnetization reversal of the nanowire, as is shown in Fig. 1b, where the stable direction of the magnetization is determined by the sign of both the in-plane field and the current, and equal to that observed in Pt/Co/$AlO_x$ (refs 23,24). This confirms that the thickest Pt layer indeed leads to a larger spin Hall current, resulting in a torque that is not fully compensated by the torque from the spin current from the thinner top layer.

We now consider the effects of this net spin Hall current on a magnetic domain wall in a nanowire. When injected into a ferromagnetic layer, the spin Hall current gives rise to a torque on the magnetization of the Slonczewski form[28]. This contribution is added to the Landau–Lifshitz–Gilbert equation, which describes the time evolution of the magnetization $M$:

$$\frac{\partial \mathbf{M}}{\partial t} = -\gamma \mathbf{M} \times \mathbf{H} + \frac{a}{M_s} \mathbf{M} \times \frac{\partial \mathbf{M}}{\partial t} - (\mathbf{u} \cdot \nabla)\mathbf{M} + \frac{\beta}{M_s} \mathbf{M} \times (\mathbf{u} \cdot \nabla)\mathbf{M} + \frac{\alpha_{SHE}}{M_s} \mathbf{M} \times (\boldsymbol{\sigma} \times \mathbf{M}) \quad (1)$$

where $M_s$ is the saturation magnetization, $\alpha$ is the Gilbert damping parameter, $\gamma$ is the gyromagnetic ratio, $\mathbf{u}$ is proportional to

Department of Applied Physics, Center for NanoMaterials and COBRA Research Institute, Eindhoven University of Technology, PO Box 513, 5600 MB Eindhoven, The Netherlands. *e-mail: pascal.haazen@gmail.com.

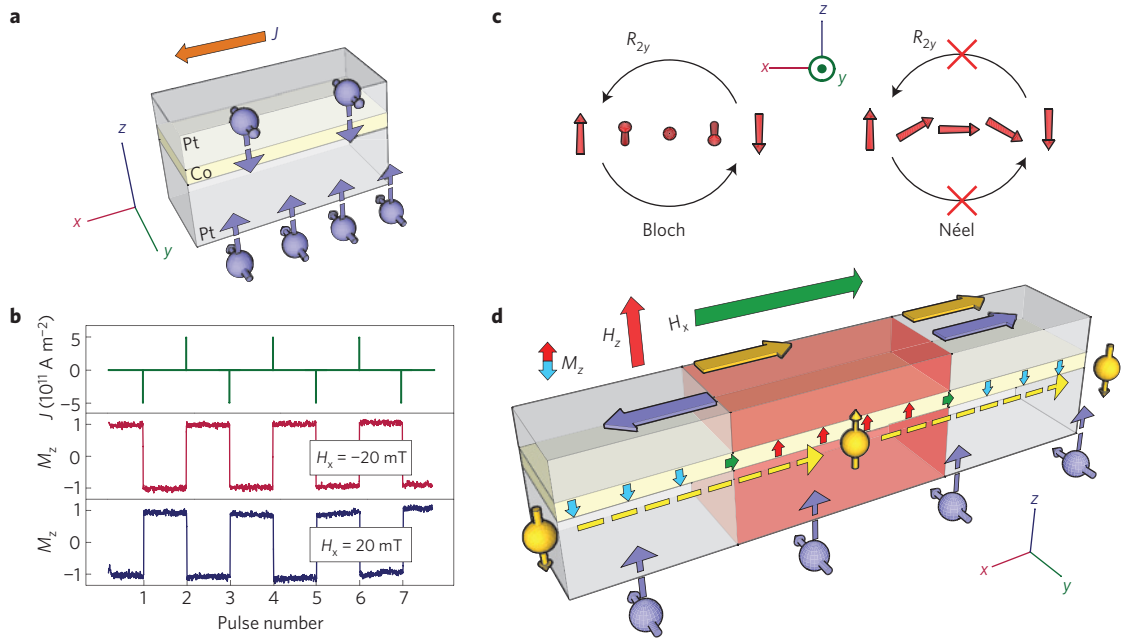


**Figure 1 | Magnetization dynamics induced by the SHE. a**, A vertical spin current is generated in both Pt layers as a consequence of the charge current density $J$ by the SHE and injected into the Co. The thickest Pt layer induces a higher spin current, leading to a non-zero net injected spin current. **b**, Perpendicular switching of a uniformly magnetized Pt (2 nm)/Co (0.5 nm)/Pt (4 nm) nanowire confirms the torque from the spin Hall current, where the combination of the charge current direction and the in-plane field $H_x$ sets the stable perpendicular magnetization direction. **c**, Bloch and Néel domain wall types. The Bloch wall is symmetric under a 180° rotation along the $y$ axis ($R_{2y}$), which prohibits motion of the domain wall when subjected to a Slonczewski torque. **d**, Contributions to the CIDWM (arrows on top of structure) from conventional gradient torques (yellow) and the SHE (violet). For simplicity, only the dominating spin current from the bottom Pt layer is visualized. Under the application of an applied magnetic field in the $x$ direction ($H_x$), the Néel wall can be stabilized, with its centre spin pointing along the field.

the charge current density, $\boldsymbol{\sigma}$ denotes the SHE spin direction and $\alpha_{\mathrm{SHE}}$ is a parameter determining the strength of the SHE. The terms on the right-hand side denote, in order, precession along an effective field $H$, the Gilbert damping, the conventional adiabatic and non-adiabatic terms, which we will refer to as gradient torques, and finally the new Slonczewski torque induced by the SHE.

To analyse the effect of the Slonczewski torque, it is important to consider the internal structure of the domain wall. As the width of the Pt/Co/Pt nanowires is much larger than the typical domain wall width, the domain walls will be of the Bloch type (Fig. 1c). For this wall type, the Slonczewski torque cannot lead to domain wall motion because of symmetry considerations: the 180° rotational symmetry around the $y$ axis ($R_{2y}$) of this wall type prohibits a well-defined direction of movement, because a hypothetical direction of motion would reverse under this symmetry operation while the system and the resulting Slonczewski torque remain unchanged. However, the Bloch wall can easily be perturbed, so that this symmetry is broken. In this research, to tune the internal structure of the domain wall, a field in the $x$ direction (along the nanowire) is applied. This applied field changes the domain wall from the initial Bloch type to a Néel type (Fig. 1c) with the centre spin aligned to the field.

When the domain wall is of the Néel type, the spins obtain an $x$ component, thereby breaking the $R_{2y}$ symmetry, which is crucial for the movement of the wall. This dependence on the $x$ component is analogous to the required tilt of the magnetization in the switching that was shown in Fig. 1b, where a specific combination of an in-plane field and spin Hall current direction results in a single stable perpendicular magnetization direction. A domain with this magnetization direction is expected to expand under the influence of the SHE (Fig. 1d, blue arrows), which we verified by micromagnetic simulations, based on equation (1) (see Supplementary Information). The adiabatic and non-adiabatic gradient terms also give rise to torques on the domain walls, and are expected to push the domain in the electron drift direction, independent of the polarity of the domain[13] (Fig. 1d, yellow arrows). Hence, one domain wall will be driven by a combination of gradient torques and the SHE because they work in parallel for that wall, whereas these two contributions counteract one another in the other domain wall, thereby providing an excellent tool to disentangle these contributions to the CIDWM.

This scheme to uniquely identify the role of the SHE is now applied to a Pt (4 nm)/Co (0.5 nm)/Pt (2 nm) nanowire, in which a well-defined region with reduced anisotropy is engineered using $Ga^+$ ion irradiation[29]. In this magnetically softer region, a domain can be stabilized, as can be seen in Fig. 2a (left panel). As the energy of a domain wall scales with the root of the anisotropy, the domain walls stay pinned at the anisotropy steps. When the perpendicular $H_z$ field is increased, a critical field $H_{\mathrm{depin}}$ will depin the domain walls over the energy barriers, after which they propagate towards the ends of the nanowire.

We now concentrate on the dependence of $H_{\mathrm{depin}}$ on an in-plane current for both domain walls where we set the Néel structure by applying an in-plane field $\mu_0 H_x = -15\,\mathrm{mT}$. As can be seen in Fig. 2b, already at reasonably low current density $J$ (that is, $\sim 10^{10}\,\mathrm{A\,m^{-2}}$), $H_{\mathrm{depin}}$ can be significantly altered, and an almost linear dependence on the current is measured. However, the observed symmetry is radically different from that expected of the conventional gradient torques. When the centre domain is magnetized in the upward direction and a negative $H_x$ is applied (Fig. 2b), a positive current results in a lower $H_{\mathrm{depin}}$ for both domain walls, and is therefore assisting the depinning of both domain walls, even though their depinning directions are opposite. When the polarity of the domain wall is reversed

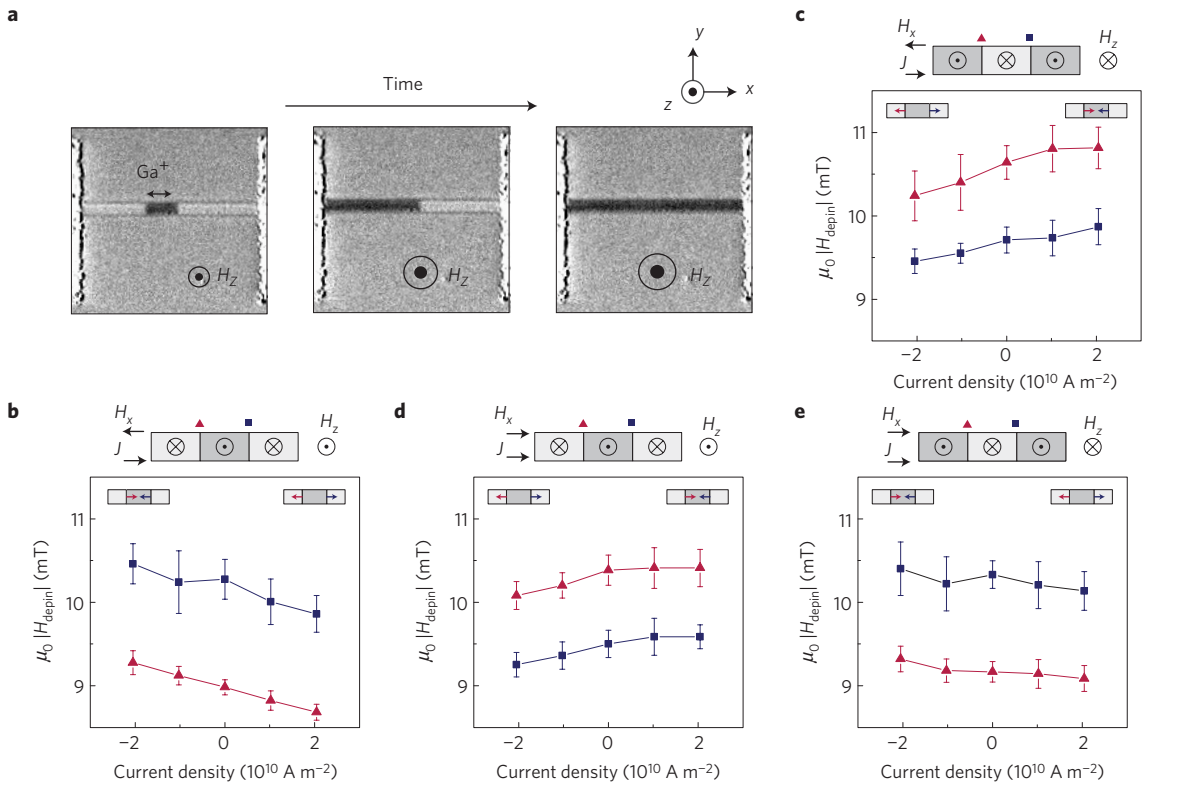


**Figure 2 | Domain wall depinning experiment. a**, Polar Kerr images of the subsequent nucleation of a domain in the low-anisotropy region and the depinning events of the two walls of the domain. **b**–**e**, Depinning fields for the right (blue squares) and left (red triangles) domain walls versus in-plane current in Pt (4 nm)/Co (0.5 nm)/Pt (2 nm). Data points are averaged values of 20 depinning events, with the standard deviation given by the error bars. Measurements were performed with in-plane fields of $\mu_0 H_x = -15$ mT (**b**,**c**) and $\mu_0 H_x = 15$ mT (**d**,**e**). The sign of the contribution of the current to the domain wall depinning changes under reversal of domain wall polarity (see **b** versus **c** and **d** versus **e**) and in-plane field (**b** versus **d** and **c** versus **e**). The schematics on top of the graphs shows the labels of the two domain walls as a legend, and the schematics in the graphs show the direction of the current-induced contribution to the depinning process for negative (left side) and positive (right side) currents.

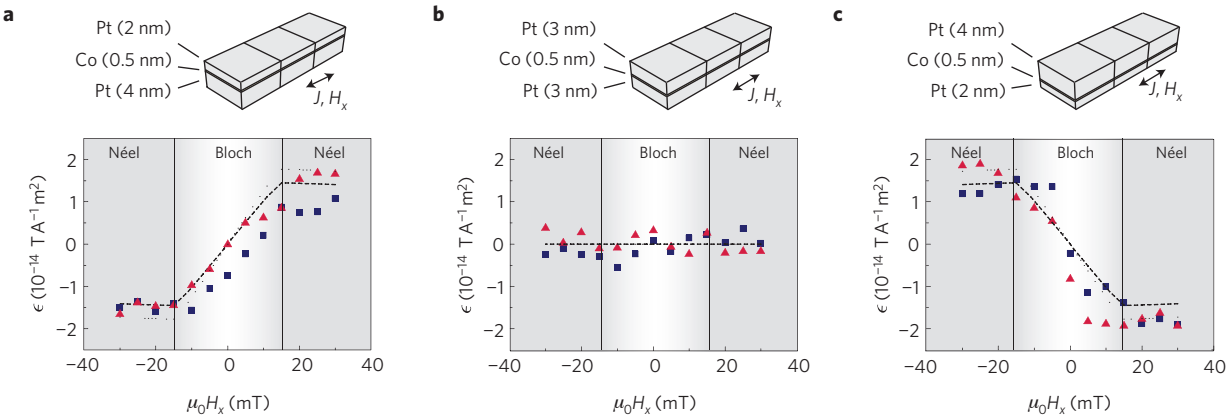


**Figure 3 | Depinning efficiency as a function of $H_x$ field, for Pt (*x* nm)/Co (0.5 nm)/Pt (*y* nm). a**, $(x,y) = (4,2)$. **b**, $(x,y) = (3,3)$. **c**, $(x,y) = (2,4)$. The magnetization of the expanding domain is parallel to $+z$. The schematics on top of the graphs indicate the stack sequence. The dashed black lines are the results of the micromagnetic simulations, performed without adjustable parameters (see Supplementary Information), and the symbols indicate $\epsilon$ for the two domain walls, with the colour coding analogous to Fig. 2. The internal structure of the domain wall, as determined by micromagnetic simulations, is indicated by the background colour of the graph. At fields higher than $\mu_0 H_x = 15$ mT, the structure is of the Néel type, and at $\mu_0 |H_x| < 15$ mT, the domain wall structure changes from the Néel type to the Bloch type (at $\mu_0 H_x = 0$ mT) to the opposite Néel type.

(Fig. 2c), the required $|H_{\mathrm{depin}}|$ increases with positive current, and the current now opposes the domain wall depinning, again for both domain walls. When the in-plane field is reversed, the slopes of $H_{\mathrm{depin}}$ versus $J$ change sign, as can be seen in Fig. 2d,e. Such behaviour cannot be explained in the conventional paradigm of gradient torques, which predicts an opposite sign of the slopes for the two domain walls, and none of the observed sign changes. Moreover, we find no systematic difference in the slopes for the two domain walls, indicating that the conventional gradient torques are negligible. Instead, we have demonstrated a new mechanism for domain wall motion, governed by the SHE. Note that the observed dependence of the depinning field at zero

current on $H_x$ and the perpendicular magnetization direction, visible as the offsets in Fig. 2b–e, is caused by the local energy landscape of the depinning centre, thereby forming a separate effect that is not relevant for the SHE behaviour of $dH_{depin}/dJ$ (see Supplementary Information).

To further prove that the SHE is of dominant importance for the domain wall depinning, we will now discuss the role of the stack composition. The subtractive nature of the two competing spin currents from the Pt layers predicts that engineering of the strength and sign of CIDWM by tuning the Pt thicknesses is possible. Therefore, we have repeated these measurements on Pt ($x$ nm)/Co (0.5 nm)/Pt ($y$ nm) nanowires with $(x, y) = (4,2); (3,3); (2,4)$. Indeed, the sign of the depinning efficiency, $\epsilon = \mu_0 \times dH_{depin}/dJ$, clearly reverses between the (4,2) and (2,4) stacks, as can be seen in Fig. 3. Furthermore, for the (3,3) stack, the two spin currents cancel, resulting in zero net spin current and no systematic influence on the domain wall depinning.

The functional dependence of $\epsilon$ on $H_x$ also shows an interesting behaviour. After a steep increase, at $\mu_0 H_x > 15$ mT, $\epsilon$ levels off for both the (4,2) and (2,4) stacks. Apart from predicting the observed linear dependence of $H_{depin}$ on current, micromagnetic simulations using only the spin-Hall-induced Slonczewski torque also reproduce this saturation, without using any free parameters (see Supplementary Information), as can be seen in Fig. 3 (dashed lines). They reveal that the internal structure of the domain wall is indeed of crucial importance for $\epsilon$. At $H_x = 0$, the domain wall is of the Bloch type, and the depinning efficiency is zero. When an $H_x$ is applied, the internal angle of the domain wall starts to align with this field, and $\epsilon$ increases. At $\mu_0|H_x| \cong 15$ mT, the domain wall is fully aligned with $H_x$ (that is, in a full Néel configuration, see Supplementary Information), and $\epsilon$ saturates. These results show that it is possible to tune the efficiency and the direction of the CIDWM by controlling the magnitude of the net spin Hall current and the internal domain wall structure.

The findings presented here have important implications for the research field, where the spread in sign and magnitude in reported values of $\epsilon$ is an urgent issue[6–11]. Owing to the abundant use of materials with high spin–orbit coupling in perpendicularly magnetized domain wall conduits, it is very likely that the SHE also plays a role in other CIDWM experiments. Even without the use of an in-plane field, deviations from a pure Bloch structure can be induced by other factors, such as field misalignments or contributions from the adiabatic and non-adiabatic torques, or from the shape anisotropy in narrow wires. Hence, it is likely that in previous research the SHE has influenced the CIDWM, and these contributions could have been erroneously ascribed to the non-adiabatic torque. We therefore believe that the SHE plays a decisive role in explaining, at least partially, the existence of contradicting reports on CIDWM in perpendicular materials.

Finally, for domain-wall-based applications, the demonstration of the SHE-driven domain wall motion offers a completely new degree of freedom for controlling domain wall motion by a charge current. We have shown that when the domain wall structure is controlled, reliable SHE-driven domain wall motion can be achieved. In narrow wires ($\lesssim$60 nm; ref. 30), the shape anisotropy favours domain walls of the Néel type, which would allow for spin-Hall-induced domain wall motion without the need for applied in-plane fields in these wires, where the initial configuration of the domain wall can be tuned to set the direction of motion. This favourable scaling behaviour makes the SHE-driven domain wall motion especially promising, because it opens up possibilities for efficient and dense data storage devices.

## Methods

The dimensions of the Pt/Co/Pt nanostrips are 1.5 μm × 20 μm × 6.5 nm. Pt and Co were deposited on thermally oxidized $SiO_x$ substrates by d.c. magnetron sputtering in a system with a base pressure of $\sim 3 \times 10^{-8}$ mbar. From these thin films, nanostrips were fabricated using electron-beam lithography and lift-off. The electrodes were made of 35-nm-thick Pt and were also deposited by sputter deposition. The out-of-plane component of the magnetization ($M_z$) of the nanostrips was measured by polar Kerr microscopy. The external magnetic field was applied in three orthogonal directions. The $H_x$ field was applied before nucleation, and kept constant until completion of the measurement routine. No contributions from Joule heating, which would have resulted in a deviation from the linear behaviour of $H_{depin}$ versus $J$, can be observed in the depinning experiments, because low current densities ($<2.5 \times 10^{10}$ A m$^{-2}$) were used.

Received 10 September 2012; accepted 17 December 2012; published online 3 February 2013

## References


1. Hayashi, M., Thomas, L., Moriya, R., Rettner, C. & Parkin, S. S. P. Current-controlled magnetic domain-wall nanowire shift register. *Science* **320,** 209–211 (2008).
2. Parkin, S. S. P. Shiftable magnetic shift register and method of using the same. US patent 6834005 (2004).
3. Honjo, H. *et al.* Domain-wall-motion cell with perpendicular anisotropy wire and in-plane magnetic tunneling junctions. *J. Appl. Phys.* **111,** 07C903 (2012).
4. Allwood, D. A. *et al.* Magnetic domain wall logic. *Science* **309,** 1688–1692 (2005).
5. Zhang, Y. *et al.* Perpendicular-magnetic-anisotropy CoFeB racetrack memory. *J. Appl. Phys.* **111,** 093925 (2012).
6. Miron, I. M. *et al.* Domain wall spin torquemeter. *Phys. Rev. Lett.* **102,** 1–4 (2009).
7. Moore, T. A. *et al.* High domain wall velocities induced by current in ultrathin Pt/Co/$AlO_x$ wires with perpendicular magnetic anisotropy. *Appl. Phys. Lett.* **93,** 262504 (2008).
8. Miron, I. M. *et al.* Fast current-induced domain-wall motion controlled by the Rashba effect. *Nature Mater.* **10,** 419–423 (2011).
9. Kim, K-J. *et al.* Electric control of multiple domain walls in Pt/Co/Pt nanotracks with perpendicular magnetic anisotropy. *Appl. Phys. Express* **3,** 083001 (2010).
10. Heinen, J. *et al.* Current-induced domain wall motion in Co/Pt nanowires: Separating spin torque and Oersted-field effects. *Appl. Phys. Lett.* **96,** 202510 (2010).
11. Lavrijsen, R. *et al.* Asymmetric Pt/Co/Pt-stack induced sign-control of current-induced magnetic domain-wall creep. *Appl. Phys. Lett.* **100,** 262408 (2012).
12. Zhang, S. & Li, Z. Roles of nonequilibrium conduction electrons on the magnetization dynamics of ferromagnets. *Phys. Rev. Lett.* **93,** 1–4 (2004).
13. Thiaville, A., Nakatani, Y., Miltat, J. & Suzuki, Y. Micromagnetic understanding of current-driven domain wall motion in patterned nanowires. *Europhys. Lett.* **69,** 990–996 (2005).
14. Berger, L. Exchange interaction between ferromagnetic domain wall and electric current in thin metallic films. *J. Appl. Phys.* **55,** 1954–1957 (1984).
15. Yamaguchi, A. *et al.* Real-space observation of current-driven domain wall motion in submicron magnetic wires. *Phys. Rev. Lett.* **92,** 077205 (2004).
16. Dyakonov, M. I. & Perel, V. I. Possibility of orienting electron spins with current. *JETP Lett.* **13,** 467–469 (1971).
17. Dyakonov, M. I. & Perel, V. I. Current-induced spin orientation of electrons in semiconductors. *Phys. Lett. A* **35,** 459–460 (1971).
18. Hirsch, J. E. Spin Hall effect. *Phys. Rev. Lett.* **83,** 1834–1837 (1999).
19. Demidov, V. E., Urazhdin, S., Edwards, E. R. J. & Demokritov, S. O. Wide-range control of ferromagnetic resonance by spin Hall effect. *Appl. Phys. Lett.* **99,** 172501 (2011).
20. Liu, L., Moriyama, T., Ralph, D. C. & Buhrman, R. A. Spin-torque ferromagnetic resonance induced by the spin Hall effect. *Phys. Rev. Lett.* **106,** 036601 (2011).
21. Kajiwara, Y. *et al.* Transmission of electrical signals by spin-wave interconversion in a magnetic insulator. *Nature* **464,** 262–266 (2010).
22. Liu, L. *et al.* Spin-torque switching with the giant spin Hall effect of tantalum. *Science* **336,** 555–558 (2012).
23. Miron, I. M. *et al.* Perpendicular switching of a single ferromagnetic layer induced by in-plane current injection. *Nature* **476,** 189–193 (2011).
24. Liu, L., Lee, O. J., Gudmundsen, T. J., Ralph, D. C. & Burhman, R. A. Current-induced switching of perpendicularly magnetized magnetic layers using spin torque from the spin Hall effect. *Phys. Rev. Lett.* **109,** 096602 (2012).
25. Seo, S-M., Kim, K-W., Ryu, J., Lee, H-W. & Lee, K-J. Current-induced motion of a transverse magnetic domain wall in the presence of spin Hall effect. *Appl. Phys. Lett.* **101,** 022405 (2012).

26. Wang, X. & Manchon, A. Diffusive spin dynamics in ferromagnetic thin films with a Rashba interaction. *Phys. Rev. Lett.* **108,** 1–5 (2012).
27. Liu, L., Burhman, R. A. & Ralph, D. C. Review and analysis of measurements of the spin Hall effect in platinum. Preprint at http://arxiv.org/abs/1111.3702v3 (2012).
28. Slonczewski, J. Current-driven excitation of magnetic multilayers. *J. Magn. Magn. Mater.* **159,** L1–L7 (1996).
29. Franken, J. H. *et al.* Precise control of domain wall injection and pinning using helium and gallium focused ion beams. *J. Appl. Phys.* **109,** 07D504 (2011).
30. Koyama, T. *et al.* Observation of the intrinsic pinning of a magnetic domain wall in a ferromagnetic nanowire. *Nature Mater.* **10,** 194–197 (2011).

## Acknowledgements

The work is part of the research programme of the Foundation for Fundamental Research on Matter (FOM), which is part of the Netherlands Organisation for Scientific Research (NWO). E.M. acknowledges support from the Swiss National Science Foundation (SNSF), Grant No. PBELP2-130894.

## Author contributions

P.P.J.H., E.M., J.H.F. and R.L. contributed to the design of the experiment. P.P.J.H. carried out the experiment with support from E.M. and J.H.F. The manuscript was prepared by P.P.J.H., together with E.M. and J.H.F., and H.J.M.S. and B.K. supervised the study. All authors discussed the results and commented on the manuscript.

## Additional information

Supplementary information is available in the online version of the paper. Reprints and permissions information is available online at www.nature.com/reprints. Correspondence and requests for materials should be addressed to P.P.J.H.

## Competing financial interests

The authors declare no competing financial interests.